SPE 84053

Modeling Facies Bodies and Petrophysical Trends in Turbidite Reservoirs

R. Hauge and A. R. Syversveen, Norwegian Computing Center, and A. C. MacDonald, Roxar ASA

This paper was prepared for presentation at the SPE Annual Technical Conference and Exhibition held in Denver, Colorado, U.S.A., 5 – 8 October 2003.

Abstract

A two-stage approach for modeling turbidite reservoirs is presented. The first stage is to model the distribution and geometry of turbidite sandbodies using an object model that can be constrained to local vector directions. The facies objects are individual turbidite sandbodies that are locally aligned to a vector parameter to model the effect of local sea-floor topography on sandbody geometry and orientation.

The second stage involves modeling petrophysical variation within each turbidite body. This is done by using a variety of intrabody trends, which describe vertical and lateral variation in the petrophysical properties. These variations are the result of grain-size and sorting trends within each turbidite sandbody.

Introduction

Sandstones deposited in deep water environments along continental margins are important oil and gas reservoirs throughout the world from West Africa to offshore Brazil and the Gulf of Mexico[1]. The sands are transported from shallow water into the deep-water depositional environments by turbidity currents. A key characteristic of these gravity driven, sediment loaded mass flows is that the local direction of flow is strongly controlled by local topographic variations on the sea floor. As a consequence of this, the geometry and orientation of turbidite sand bodies closely reflect paleo-topographic features[2].

Object models are often applied to modeling of reservoir architectures where the facies geometry is relatively well defined. Such models were initially adopted for modeling channel-like geometries in fluvial reservoirs.[3,4,5] Subsequently, a variety of facies morphologies have been modeled in a large number of fields using general object models like the one given in[6].

These general models have also been successfully applied to turbidite reservoirs[7]. In such reservoirs, however, local paleotopographic variations can create complex variation in sandbody orientation and local reservoir connectivity.

The object model described by[6] has been extended in order to describe such local variations in sandbody orientation. This has been achieved by introducing objects with a flexible shape which is built around a piecewise linear centerline, called the backbone. Similar ideas have been used to create meandering channels.[5] However, in order to recreate topographic features, the ability to condition this backbone to a vector field is introduced here. This vector field may be two- or three-dimensional, and can be extracted from the structural interpretation of the reservoir, isochore information or directly from seismic data.

Another key feature of turbidity flows is that there is a systematic segregation of grain-sizes within the flow[8]. This segregation results in the characteristic upward-fining signature of turbidite sandbodies. It also produces systematic proximal to distal fining of grain-sizes and a lateral fining of grain-sizes from the axis to the margins of flows.

These systematic variations in grain-size and sorting produce corresponding variations in porosity and permeability. Using an object model provides a framework for incorporating these important trends in the reservoir model. Petrophysical properties can be simulated separately for each turbidite body in a coordinate system defined along the centerline. Anisotropies follow the local direction of the backbone. Petrophysical trends are related to position within the bodies. A complex set of coordinate transforms, described in[9], is used to ensure that both facies and petrophysical well data are correctly honored, and to map the locally generated petrophysical values into the reservoir.

Facies model

The turbidite sand bodies are modeled as objects that are placed in a background of shale. The model is based on the approach described in[6]. This is a marked point process model, where the object locations are the points, and the marks describe the object geometry.

An intensity trend controls the location of objects. Each object has a reference point at a given location in the object. The likelihood of this point being at a certain location is proportional to the intensity there. The total number of objects is controlled by a volume fraction. Interaction between objects is introduced through repulsion between reference points.

This paper describes a modification to the treatment of body orientations in the model described in[6]. In the original model, the expected (mean) values for azimuth and dip angles can be constants or can be defined by a variety of 1D, 2D or

3D trends. A variability in orientation (standard deviation) is also defined so that, at any point in the reservoir, body orientation is defined by a normal distribution with an expected value and a standard deviation.

The orientation of each individual object is drawn from the azimuth and dip parameter distributions at the position of the object's reference point as illustrated in Figure 1. Each object is assigned a single global orientation.

This algorithm has proved to be suitable for modeling body orientations that are controlled by large-scale regional paleoslopes and paleogeographc features. For relatively small facies bodies it has also proved successful for modeling more local effects. For large, continuous facies bodies, however, the original algorithm[6] cannot be used to model the local variations in orientation along single bodies.

A new type of object, called backbone, has therefore been introduced. As with the conventional object type, the orientation of a backbone object, at any point in the reservoir, is defined by a normal distribution with an expected value and a standard deviation. Unlike conventional objects the orientation is defined locally as illustrated in Figure 1.

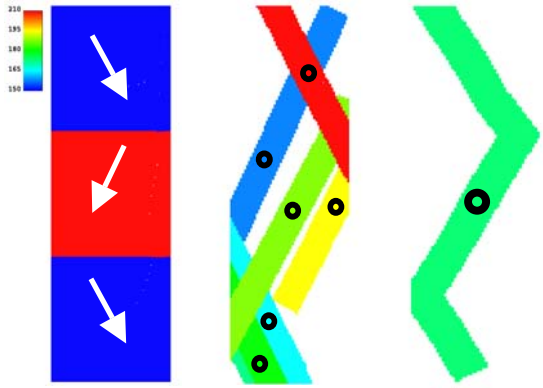

Vector field Conventional Backbone

Figure 1: Example of 2D azimuth parameter (mean values), and how conventional and backbone objects are conditioned to the varying azimuths.

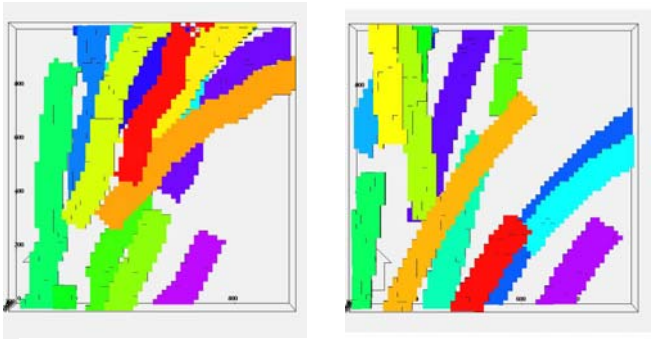

Large flexibility Small flexibility

Figure 2: Effect of flexibility parameter.

The backbone object is parameterized around a piecewise linear centerline, where each piece has an expected local rotation and dip given by the vector field. The vector field may be 2 or 3 dimensional. The additional parameters for the backbone object are the length of the pieces and a flexibility parameter. Low values of the flexibility will result in smooth objects where all pieces have the same deviance from the vector field, whereas a large value allows more oscillation around the expected direction. This is illustrated in Figure 2. The details of this conditioning are given in[9].

The idealized shape of the objects is defined by independent trends for thickness along and across this centerline, together with a width trend along the line. Each object has its own height, width and length drawn from a distribution, and the trends are scaled proportionally for objects of different size.

Local variations from the idealized form are given by a set of Gaussian fields. Along the centerline, 1D fields are added to the right and left edges, allowing local changes in width. In addition, 2D Gaussian fields are added to the top and bottom of the object. As with other object models[10], these local variations are introduced to allow for exact well conditioning, especially when one object passes through several wells.

A Metropolis-Hastings algorithm is used to create realizations from this model. This is an iterative algorithm, which makes a proposed new state in each iteration, and then accepts or rejects it based on the likelihood under the model. Each proposal consists of either adding, removing or changing one object. The termination criteria are that a certain minimum number of iterations have been run, and that the volume fraction of objects is satisfied. To ensure the honoring of the volume fraction, simulated annealing is used. Simulated annealing works by allowing a wide range of values initially, but restricting towards the target as the number of iterations increase.

Well conditioning is handled by placing objects close to wells and drawing their parameters conditioned on observations in wells they pass through. All well intersections are assumed to be through the top or bottom of the objects, and the 2D Gaussian fields are used to produce exact match. Many objects are proposed, and a Metropolis-Hastings algorithm is used to choose between them, so that the model is honored. For further details on well conditioning, see[6]. This model can also condition on seismic data[11].

Petrophysical model

A transformed Gaussian field approach is used for the petrophysical model, and conditioned to well data using kriging. This is a classical approach. However, the conditioning on the facies realization is taken one step further here by utilizing object information. Instead of creating one field for each facies, a separate field is created for each object. Furthermore, these fields are generated in a straightened version of the object, where the centerline is a straight line. This grid is then bent into shape, as seen in Figure 3. This figure shows how the grid cells are deformed in this process. Values in the grid cells remain the same throughout the bending. This approach automatically creates anisotropy that follows the shape and local orientation of the object, as well as erosion effects in the petrophysical field, as seen in Figure 4.

In addition to the local anisotropy, the body co-ordinates can used to create intrabody trends. These trends depend on the distance to the edge of the object, either horizontally or vertically. In a horizontal direction, the trends can be along or across the axis of the object (Figure 5). 1D Trends in different

directions can be combined to produce 2D and 3D trends, but the component 1D trends are always independent.

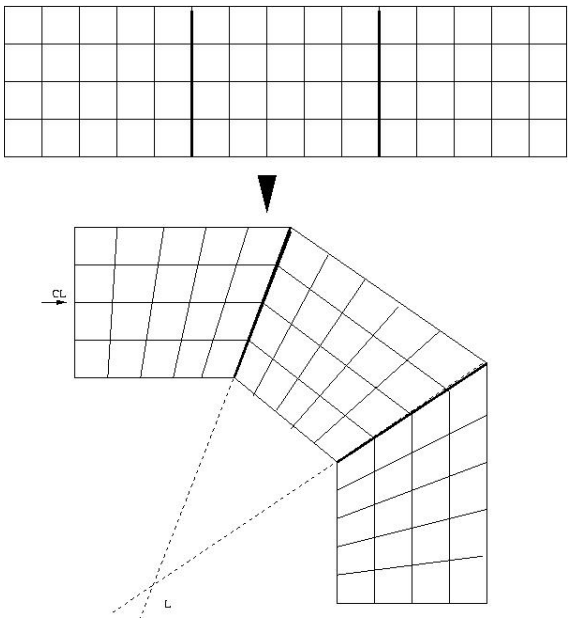

Figure 3: Mapping from straightened to real world coordinates.

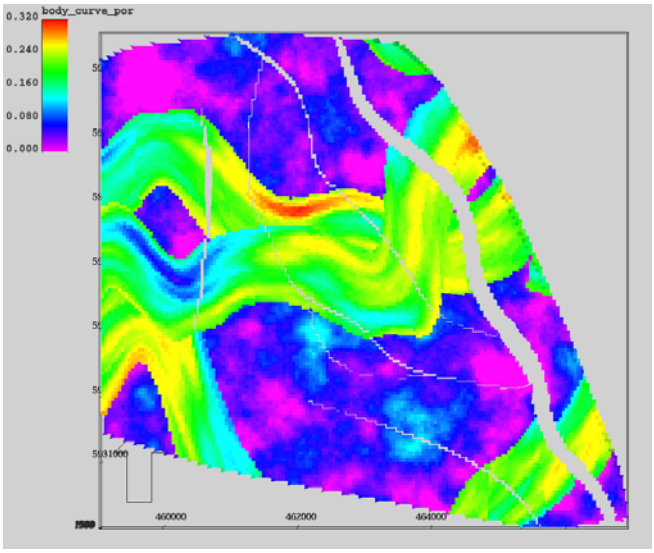

Figure 4: Local anisotropy of porosity in a channel reservoir. Note how the anisotropy follows the curvature, and the erosion between channels.

Synthetic "Gulf of Mexico" example

The two stage modeling procedure and the application of backbone objects and intrabody petrophysical trends is illustrated using a synthetic example based on a turbidite reservoir in the Gulf of Mexico. A synthetic reservoir has been generated using an unconditional simulation based on the volume fraction trends, facies thickness statistics, and porosity statistics from the field. Six wells have then been placed in the synthetic reservoir and the well data, along with a synthetic structural framework have been used to test and illustrate the modeling algorithms. The modeling area is 3x9 km^2.

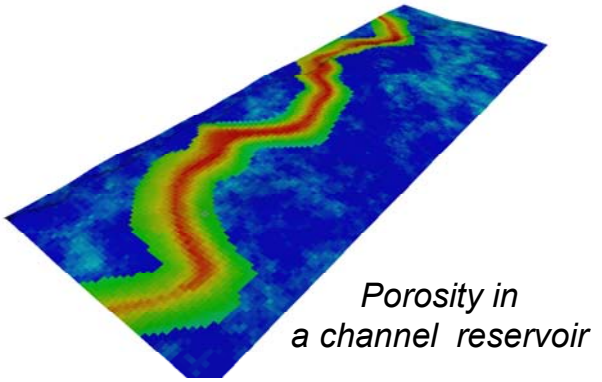

Figure 5: Porosity intrabody trend in channel. The trend across the axis produces high porosities along the axis and lower values towards the margin.

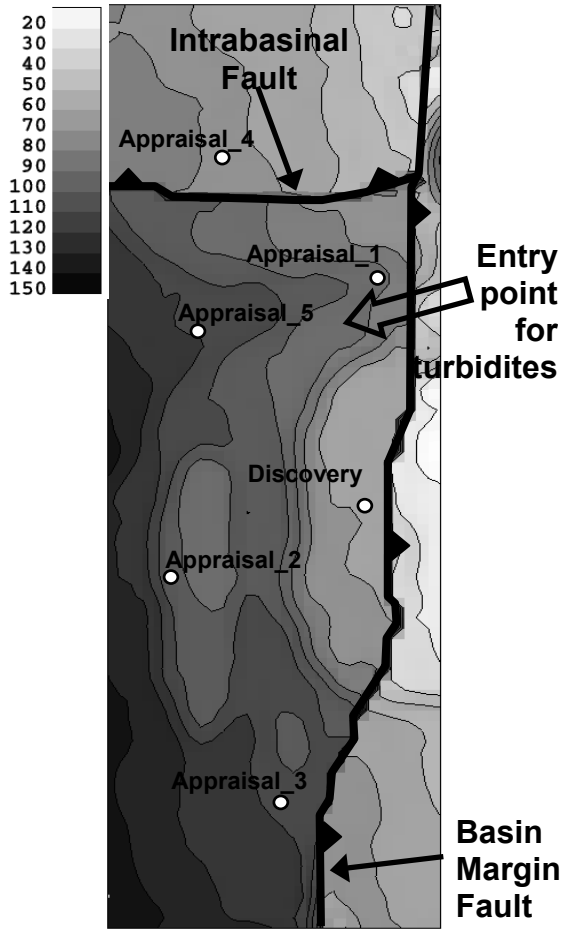

Figure 6: Isochore and location map. Map is 3x9 km^2.

Reservoir structure. The field is bounded by a major N-S trending, high angle reverse fault to the East, shown in Figure 6. This fault was active during turbidite deposition. The reservoir was deposited in a sub-basin to the West of this major fault and is cut by one significant W-E oriented intrabasinal fault, which was also active during deposition. The stratigraphic interval of the reservoir varies in thickness

from 30 to 150 m. The isochore of the reservoir interval is interpreted to reflect the basin floor topography. Six exploration and appraisal wells have been drilled. Their locations are shown in Figure 6.

Well data and facies interpretation. The well data comprise stacked and single turbidite sandbodies that are up to 6 m thick, as seen in Figure 7. The NTG is highly variable with a range from 0.75 to 0.12 in the 6 wells. Two of the wells comprise stacked turbidite sandstones whereas the other four are generally characterized by single turbidite sandstone beds with only occasional stacking. The porosity logs are characterized by the typical upwards decreasing porosity motif that is reflecting grain-size and sorting variation in the turbidite sandbodies.

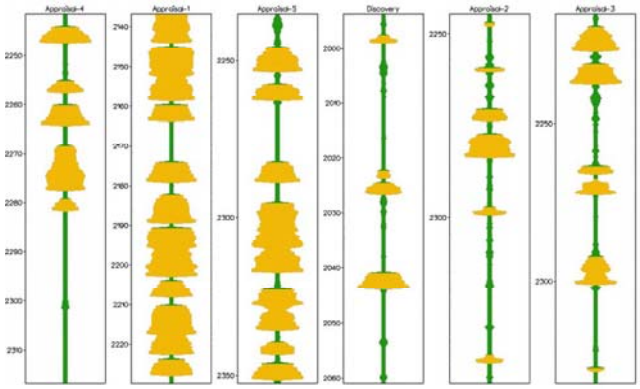

Figure 7: Mirrored porosity logs. Light grey is sand, dark grey is shale. Logs are flattened on top and base reservoir picks.

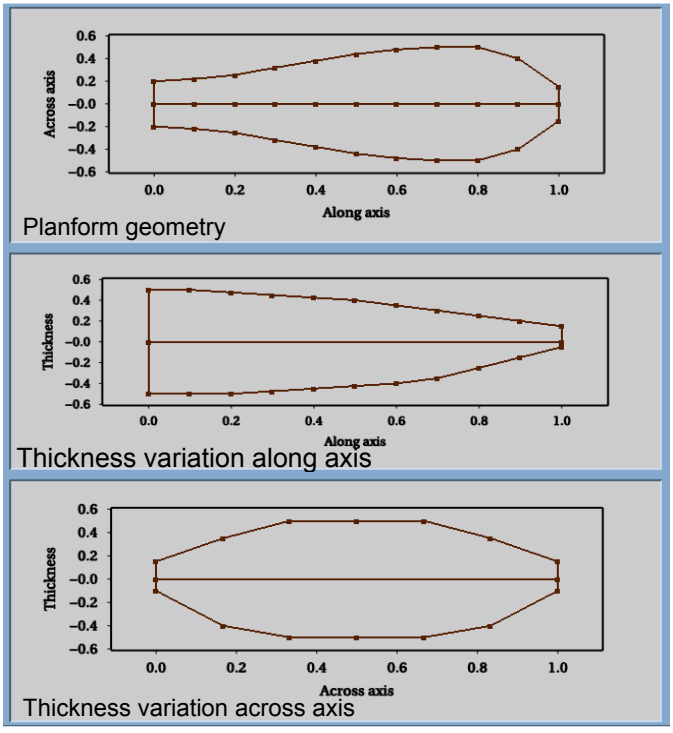

Figure 8: Definition of turbidite body - idealized shape.

It is difficult to identify classical turbidite channel and lobe facies associations from the well data. The sandbodies have been interpreted to reflect large-scale and prolonged turbidity current events. The stacking of sandbodies in the Appraisal_1 and Appraisal_5 wells is interpreted to reflect a topographic confinement and focusing of the turbidity flows related to a structurally controlled entry point into the sub-basin. This entry point has been interpreted based on the well data and a local thickness increase in the isochore in Figure 6.

Object shape. The idealized shape of the turbidite bodies is defined by three geometric profiles as in Figure 8. In map view the turbidite body is relatively narrow and confined near its proximal end, becomes gradually wider along its length and then narrower near its distal termination. Body thickness gradually decreases along the length of the body from the proximal to distal end. The turbidites have a lensoid geometry normal to the main flow direction. This includes a lower, erosional channel-like form and an upper depositional mounded geometry.

An example of a single simulated turbidite body is illustrated in Figure 9. The simulated body geometry is a combination of the idealized shape and local variations from the idealized shape as described earlier.

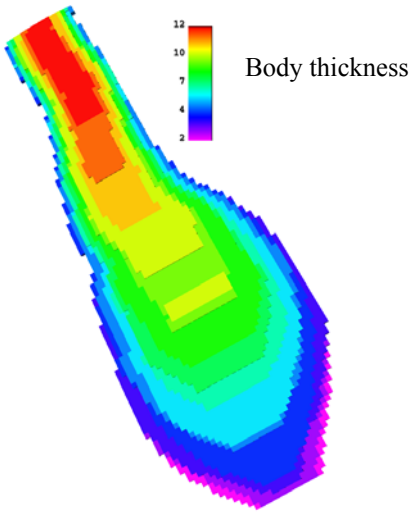

Figure 9: Example of a single simulated turbidite body. Body thickness is color coded.

Object dimensions. The lateral dimensions of turbidite bodies are dependent on a large number of factors including the dimensions of the turbidity flow, the grain-sizes in the flow, slopes and degree of confinement. As a result the dimensions are highly variable in different depositional settings and sub basins. Most turbidite sandbodies are however several km to several 10's of km long and many sand beds are often field-wide. In this example the lengths of the turbidities were assumed to vary between 4 and 10 km and the widths were up to 3 km. These estimates were mainly based on an analysis of the well data, which suggest significant lateral discontinuity.

Confined entry point. The geological interpretation, based on the well data and the isochore, is that the turbidites were fed into the basin through a single, relatively constricted entry point from the West (Figure 6). In order to reflect this process, an intensity field with a high intensity region was

generated using the isochore information. This high intensity region is then used to seed the locations of the turbidite sandbodies. This is achieved by placing the reference point for the turbidite sandbodies near to the proximal end and by setting object intensities to zero away from the high intensity region. All reference points must therefore be simulated in the area of high intensity and this ensures that all turbidite bodies will be sourced through the focused entry point. This is illustrated in Figure 10.

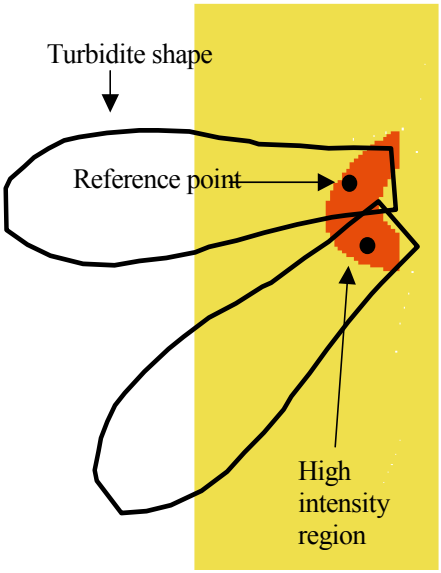

Figure 10: Modeling the confined entry point. All turbidite bodies will be "seeded" in the high intensity region. This is used to mimic the topographic control on the entry point for the turbidites into the sub-basin.

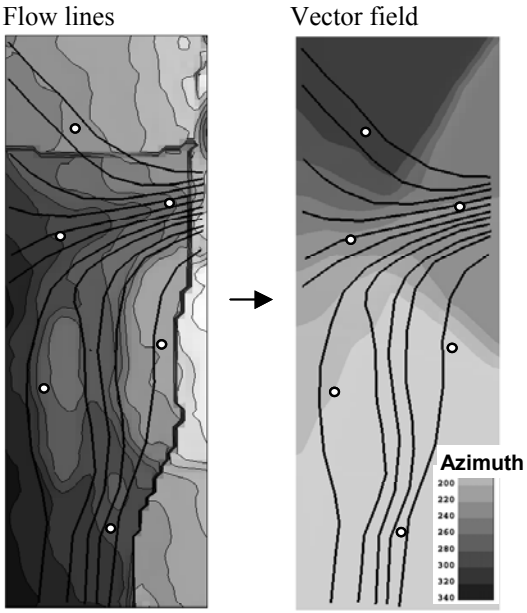

Figure 11: Vector field generated from flow lines. Flow lines are digitized based on the isochore. The vector (azimuth) field is generated using the flow lines.

Body orientation. The local orientation of the turbidite bodies is defined by a 2D vector (direction) field. The vector field has been generated based on manually interpreted and digitized flow lines, as seen in Figure 11. The interpreted flow lines are based on the geologist's interpretation, the assumption of a confined entry point, and local variations in the isochore, which are thought to reflect paleotopography. Lines starting within the high intensity region spread out in all directions, and since the bodies are conditioned on this field, they will do the same.

Body repulsion and compensational offset. Statistical pointwise repulsion has been applied to model compensational stacking effects, which are very typical for turbidite sand-bodies. Pointwise repulsion is applied to the reference points, which are placed in the high intensity area as shown in Figure 10. This ensures that reference points cannot be simulated very close to each other in the vertical and horizontal directions. The combination of a simple pointwise repulsion coupled with the conditioning to the vector field produces realistic compensational offset stacking patterns. The reason this works so well is that even a small horizontal perturbation at the starting point will take the body in an entirely different direction through the vector field.

3D facies architecture. Conditional facies realizations have been generated using the synthetic well data and the input parameters described above. Cross sections through a single realization of facies architecture are shown in Figure 12. The realization comprises 32 sandbodies. The figure illustrates realistic geometries for this type of turbidite reservoir. In proximal areas, near the entry point in the east, the turbidite sandbodies are confined and vertically stacked. The reservoir becomes increasingly layered in more distal areas toward the west.

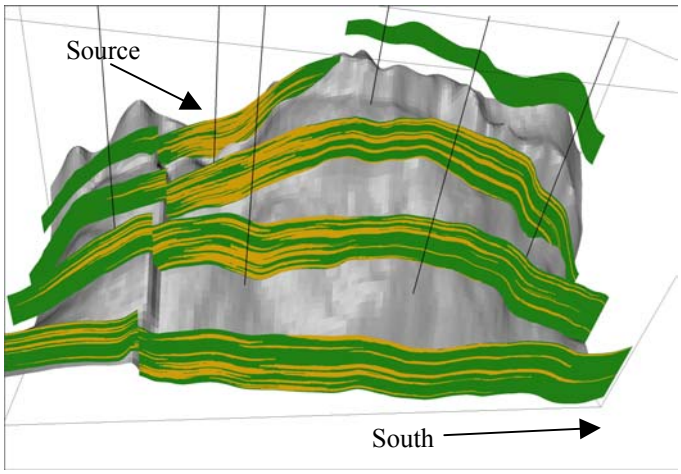

Figure 12: Cross sections of conditional realization seen from west.

A variety of geometries are apparent in the N-S oriented cross-sections. Some of the sandbodies are lensoid/discontinuous, whereas others are very continuous. These apparent dimensions are actually related to sandbodies in different orientations; the continuous sandbodies in the southern part of

the cross-sections are oriented N-S due to the vector field values (Figure 11), and are parallel to the cross-sections, whereas the apparently more discontinuous sandbodies in the central part of the field have an E-W orientation as defined by the vector field.

Porosity modeling. Significant upwards decreasing porosity trends can be clearly seen in the well data in Figure 7. These trends reflect the classical upward fining trend for turbidite bodies. Some thin high porosity streaks are also observed at the base of some of the turbidite beds and are related to thin, coarser grained lags. A piecewise linear porosity trend, shown in Figure 13, has been used to capture the overall upwards deceasing porosity and the basal high porosity streak.

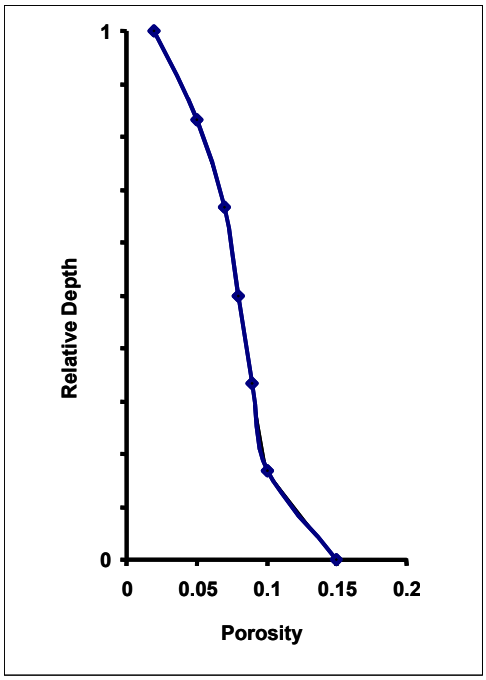

Figure 13: Vertical piecewise linear porosity trend.

It is more difficult to identify lateral porosity trends using the well data. The more distal wells in the South have, however, generally lower porosity than the wells that are nearer to the focused entry point. There is also a relatively clear relationship that the thinner beds tend to be lower porosity than the thicker beds. Two lateral trends were applied: A piecewise linear axial-margin trend, with porosity decreasing abruptly towards the margin of the sandbodies, and a linear proximal-distal trend with gradually decreasing porosity towards the distal termination of the sandbodies.

Variability around these porosity trends is modeled using a variogram with long correlation lengths (4000 m) parallel to the local body orientation and shorter correlation lengths (500 m) normal to the local body orientation. Vertical correlation lengths were set to 2m. The standard deviation of the porosity is 0.025.

The combined effects of the three 1D trends and the anisotropic variograms are illustrated in Figure 14 and Figure 15. In Figure 14, the porosity clearly decreases along the length of the turbidite sandbodies. The axial parts of the sandbodies have generally higher porosity than the margins. Also note that the regions of high and low porosity values follow the local body alignment.

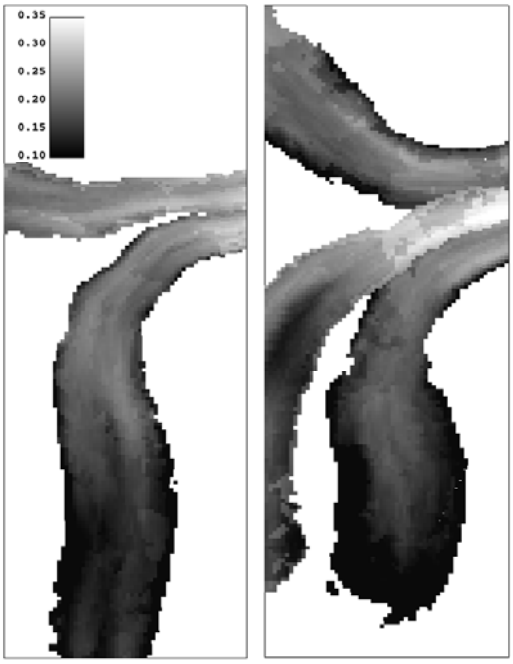

Figure 14: Two horizontal slices through 3D realization, showing the horizontal intrabody trends.

The three North-South oriented cross-sections in figure 15 illustrate how the reservoir architecture changes character from a constrained set of high-porosity stacked channels in the East to thin, layered lobes with lower porosity towards the West and South. The general decrease in porosity from East to West and towards the South is a large-scale and consistent proximal-to-distal trend that is a direct result of decreasing grain-sizes in the turbidites.

Lateral and vertical intrabody trends are also observed in Figure 15.

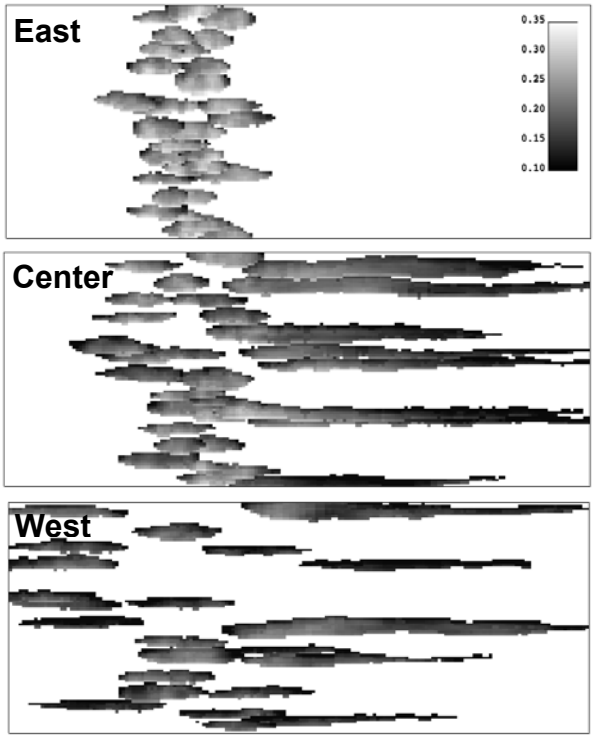

Figure 15: Porosity in three north-south cross sections.

Concluding remarks

Vectorial steering of local body orientation is necessary for producing realistic reservoir models for topographically controlled turbidite reservoirs. The approach introduced in this paper allows for such vectorial steering constrained to well information. The method can also be used to constrain sandbody distribution to seismic data.

Petrophysical properties in turbidite reservoirs are characterized by a general lack of stationarity. This paper presents an application of realistic intrabody trends to account for such non-stationarity.

The general reservoir architecture of the test example comprises a constrained set of high-porosity stacked channels in the East, which gradually evolve into a less stacked and more layered system with lower porosity in the West and South. The combination of the local steering of body alignment and the intrabody trends produces very realistic facies and porosity architectures for this type of turbidite reservoirs.

The realistic modeling of such architectures also provides an improved basis for volumetric calculations and development planning using flow simulators.

References

1. P.Weimer, *et al.,* eds, *GCSSEPM Foundation 20th Annual Research Conference. Deep-Water Reservoirs of the World*, December 3-6, 2000.
2. B.E. Prather, J.R. Booth, G.S. Steffens, P.A. Craig, "Classification, lithologic calibration, and stratigraphic succession of seismic facies of intraslope basins, deep-water Gulf of Mexico"*, AAPG Bulletin*, Vol **82**, pp 701-728, 1998.
3. C. Deutsch, L. Wang, "Hierarchical Object Based Stochastic Modeling of Fluvial Reservoirs", *Mathematical Geology*, Vol **28**, pp. 857-880, 1996.
4. L. Holden, R. Hauge, O Skare, A. Skorstad, "Modelling of Fluvial Reservoirs with Object Models", *Mathematical Geology*, Vol. **30**, pp. 473-496, 1998.
5. S. Viseur, A. Shtuka, J. Mallet, "New Fast, Stochastic, Boolean Simulation of Fluvial Deposits", 1998 Annual Technical Conference and Exhibition, paper no. 49281, Soc.of Pet. Eng., pp. 697-709.
6. O. Lia, H. Tjelmeland, L. Kjellesvik, "Modelling of Facies Architecture by Marked Point Models", In E. Baafi & N. Shofield, eds, *Geostatistics Wollongong '96*, Vol 1, Kluwer Academic Publishers, pp. 386-397.
7. K. Yang, J. M. Yarus, W. P. Catanese, "Characterization and 3-D Modeling of Turbidite Reservoir: A Case Study in Miocene Slope Deposits, Main Pass Area, Offshore Gulf Coast of Mexico", In Gulf Coast Association of Geol. Soc. Lafayette, Louisiana, sept. 15.-17. 1999, pp 54-61.
8. D.A.V. Stow, H.G. Reading, J.D. Collinson, "Deep Seas", In H.G. Reading, *Sedimentary Environments, Processes, Facies and Stratigraphy*, Blackwell Sciences, p 395-453, 1996.
9. R. Hauge, A. MacDonald, A. Syversveen, "Object Models with Vector Steering", NR note SAND/01/03, Norwegian Computing Center May 2003.
10. J. Wang, A.C. MacDonald, "Modeling Channel Architecture in a Densely Drilled Oilfield in East China", SPE 38678. 1997 Annual Technical Conference and Exhibition, p 365-372
11. O. Lia, J. Gjerde, "A marked point process model conditioned on inverted seismic data", in *IAMG '98 Proceedings of the Fourth Annual Conference of the International Association for Mathematical Geology*, October 1998, pp. 794-799.